From Miami to Madison: Investigating the relationship between climate and terrestrial net primary production

David P. M. Zaks,[1] Navin Ramankutty,[1,2] Carol C. Barford,[1] and Jonathan A. Foley[1]

Received 6 February 2006; revised 28 March 2007; accepted 4 May 2007; published 20 July 2007.

[1] The 1973 "Miami Model" was the first global-scale empirical model of terrestrial net primary productivity (NPP), and its simplicity and relative accuracy has led to its continued use. However, improved techniques to measure NPP in the field and the expanded spatial and temporal range of observations have prompted this study, which reexamines the relationship of climatic variables to NPP. We developed several statistical models with paired climatic variables in order to investigate their relationships to terrestrial NPP. A reference data set of 3023 NPP field observations was compiled for calibration and parameter optimization. In addition to annual mean temperature and precipitation, as in the Miami Model, we chose more ecologically relevant climatic variables including growing degree-days, a soil moisture stress index, and photosynthetically active radiation (PAR). Calculated annual global NPP ranged from 36 to 74 Pg-C yr^{-1}, comparable with previous studies. Comparisons of geographic patterns of NPP were made using biome and latitudinal averages.

Citation: Zaks, D. P. M., N. Ramankutty, C. C. Barford, and J. A. Foley (2007), From Miami to Madison: Investigating the relationship between climate and terrestrial net primary production, *Global Biogeochem. Cycles*, *21*, GB3004, doi:10.1029/2006GB002705.

1. Introduction

[2] A key component of the terrestrial carbon cycle is net primary productivity (NPP), the net rate at which plants assimilate carbon through photosynthesis and lose carbon through autotrophic respiration [*Clark et al.*, 2001a]. NPP also serves as an index of energy flow through ecosystems [*Roxburgh et al.*, 2004] and of ecosystem function [*Schlapfer and Schmid*, 1999]. An improved understanding of the factors that determine NPP can be valuable in reducing the level of uncertainty in the global carbon balance. Moreover, knowledge about the spatial distribution of NPP across the globe is useful in monitoring anthropogenic impacts on the terrestrial carbon cycle and associated changes in the goods and services delivered by ecosystems [*Cramer and Field*, 1999; *Haberl et al.*, 2004; *Meyerson et al.*, 2005; *Vitousek et al.*, 1997].

[3] NPP is a flux that cannot be observed directly, but is often modeled or extrapolated from field measurements of other related quantities. NPP observations, as referred to in this paper, are the relevant aboveground and belowground fluxes of organic materials that are measured or estimated from field studies [*Clark et al.*, 2001a; *Gower et al.*, 2001, 1999; *Scurlock et al.*, 2002]. While there is not yet a standardized methodology for measuring NPP, this study assumes a relative amount of accuracy from figures published in the literature. While observation-derived estimates are continuing to accumulate across many regions of the world [*Clark et al.*, 2001b; *Malhi et al.*, 2004; *Olson et al.*, 2001; *Scurlock et al.*, 1999], there is still no globally continuous data set of observed NPP. Previous studies that estimated global patterns of NPP have ranged from simple empirical models [*Lieth*, 1973; *Lieth and Whittaker*, 1975; *Rosenzweig*, 1968; *Whittaker and Likens*, 1975] to fairly complicated process-based ecosystem models [*Cramer and Field*, 1999; *Foley*, 1994; *Foley et al.*, 1996; *Haxeltine and Prentice*, 1996; *Kucharik et al.*, 2000]. The simple logic of empirical models yields reasonable results, but lacks mechanistic processes such as canopy and soil physics and plant physiology utilized in process-based models [*Foley et al.*, 1996; *Kucharik et al.*, 2000; *Running et al.*, 2004; *Sitch et al.*, 2003; *Zhao et al.*, 2005]. Nevertheless, empirical models have proved useful.

[4] The Miami model [*Lieth*, 1973; *Lieth and Whittaker*, 1975] was one of the first global empirical models; its simplicity and relative accuracy have led to its continued use. It utilizes empirical functions of mean-annual temperature and annual precipitation fitted to observations of NPP that were available in the early 1970s. The Miami model determines NPP for a particular location as the minimum of the temperature and precipitation functions. Hence there are no interactions between the two variables, and temperature and moisture are not linked. This type of model must be reparameterized with observation-based data if new sets of productivity and climate observations are used, and therefore its usefulness in climate change studies is limited [*Adams et al.*, 2004]. Nevertheless, its relative simplicity

[1]Center for Sustainability and the Global Environment (SAGE), Nelson Institute for Environmental Studies, University of Wisconsin, Madison, Wisconsin, USA.

[2]Department of Geography, McGill University, Montreal, Quebec, Canada.

0886-6236/07/2006GB002705

Table 1. Primary Literature Sources for Data Used in This Study

Data Source	Dates	Number of Records	Citation or URL
BigFoot Validation	1999–2003	7	*Turner et al.* [2005]
RAINFOR	1956–2002	104	*Malhi et al.* [2004]
ORNL NPP Boreal Forest: Canal Flats, Canada	1984	4	http://www.daac.ornl.gov
ORNL NPP Boreal Forest: Consistent Worldwide Site Estimates	1977–1994	24	http://www.daac.ornl.gov
ORNL NPP Boreal Forest: Flakaliden, Sweden	1986–1996	5	http://www.daac.ornl.gov
ORNL NPP Boreal Forest: Jadraas, Sweden	1973–1980	2	http://www.daac.ornl.gov
ORNL NPP Boreal Forest: Kuusamo, Finland	1967–1971	1	http://www.daac.ornl.gov
ORNL NPP Boreal Forest: Siberian Scots Pine Forests, Russia	1968–1974	14	http://www.daac.ornl.gov
ORNL NPP Boreal Forest: Superior National Forest, USA	1983–1984	63	http://www.daac.ornl.gov
ORNL NPP Grassland: NPP Estimates From Biomass Dynamics For 31 Sites	1948–1996	11	http://www.daac.ornl.gov
ORNL NPP Grassland: Vindhyan, India	1986–1989	12	http://www.daac.ornl.gov
ORNL NPP Multi-Biome: Global Primary Production Data Initiative Products- Class A Sites	1931–1996	161	http://www.daac.ornl.gov
ORNL NPP Multi-Biome: Global Primary Production Data Initiative Products- Class B Sites	1931–1996	2197	http://www.daac.ornl.gov
ORNL NPP Multi-Biome: Grassland, Boreal Forest, and Tropical Forest Sites	1939–1996	49	http://www.daac.ornl.gov
ORNL NPP Multi-Biome: Pik Data For Northern Eurasia	1940–1988	117	http://www.daac.ornl.gov
ORNL NPP Multi-Biome: Vast Calibration Data	1965–1998	181	http://www.daac.ornl.gov
ORNL NPP Temperate Forest: Great Smoky Mountains, Tennessee, USA	1978–1992	8	http://www.daac.ornl.gov
ORNL NPP Temperate Forest: Humboldt Redwoods State Park, California, USA	1972–2001	8	http://www.daac.ornl.gov
ORNL NPP Temperate Forest: Otter Project Sites, Oregon, USA	1989–1991	6	http://www.daac.ornl.gov
ORNL NPP Tropical Forest: Chamela, Mexico	1982–1995	3	http://www.daac.ornl.gov
ORNL NPP Tropical Forest: Cinnamon Bay, U.S. Virgin Islands	1982–1993	1	http://www.daac.ornl.gov
ORNL NPP Tropical Forest: Consistent Worldwide Site Estimates	1967–1999	34	http://www.daac.ornl.gov
ORNL NPP Tropical Forest: John Crow Ridge, Jamaica	1974–1978	5	http://www.daac.ornl.gov
ORNL NPP Tropical Forest: Luquillo, Puerto Rico	1963–1994	9	http://www.daac.ornl.gov
ORNL NPP Tropical Forest: San Carlos De Rio Negro, Venezuela	1975–1984	5	http://www.daac.ornl.gov
ORNL NPP Tundra: Toolik Lake, Alaska	1982	4	http://www.daac.ornl.gov

and ability to generate reasonable global patterns of NPP is attractive. The empirical approach has proven effective in past studies, and here we aim to provide updated global maps of NPP using more than 50 times as much data as the original model.

[5] Limited work has been done to test the control of multiple environmental variables over global patterns of NPP [*Adams et al.*, 2004]. In particular, it is well known that plants respond to the seasonality of climate, and therefore it would be useful to examine the relationship between NPP and biophysical variables that account for seasonality. Moreover, the availability and quality of global-scale gridded climate data has greatly improved since previous attempts to model NPP. *New et al.* [2002] have developed finer spatial resolution climate data sets (10 minutes in latitude by longitude), an improvement over previous data sets (0.5 to 5 degrees), allowing for a better match in scale between the climate data sets and site-level NPP data. Finally, since the earlier work of *Lieth* [1973] that used 52 field-based observations of NPP, the available data on NPP has expanded to include thousands of sites from different climates and biomes.

[6] In this paper, we develop a suite of empirical models in order to examine the relationships between several ecologically related climatic variables and a global compilation of 3023 observationally derived estimates of NPP for natural vegetation types. These observations represent a range of climates, from hot and wet to cold and dry. We further use the empirical model to spatially extrapolate the NPP observations to the globe using observed global climate data. We explore potential environmental drivers of NPP using process-based models of photosynthetically active radiation (PAR) to represent light, growing degree-days (GDD) to represent seasonal heat accumulation, and evapotranspiration or soil moisture to represent water availability.

[7] These empirical global-scale NPP estimates may be used to improve understanding of environmental controls on global-scale NPP, help understand how NPP might have been altered by land use [e.g., *DeFries et al.*, 1999], and assess the human appropriation of net primary productivity [*Cramer et al.*, 1999, 2001b; *Haberl et al.*, 2004; *Vitousek et al.*, 1997]. In addition, comparing the resulting maps of this study with the NPP output of process-based ecosystem models can assist in model development and evaluation. Determining the current state of terrestrial productivity is also important for global environmental agreements such as the Kyoto Protocol [*Cramer et al.*, 2001a; *Steffen et al.*, 1998] and future climate-related polices [*Benitez et al.*, 2007].

2. Observations of NPP

[8] The limited network of NPP observations has inhibited previous estimates and models from coming to a consensus on the global distribution of NPP [*Cramer and Field*, 1999; *Cramer et al.*, 1996; *Scurlock et al.*, 1999]. Nevertheless, the development of improved techniques to measure NPP in the field [*Clark et al.*, 2001a; *Gower et al.*, 2001, 1999; *Scurlock et al.*, 2002] and the expanded spatial and temporal range of observations has prompted our attempt to evaluate global-scale NPP patterns. A large reference data set (n = 3023) of NPP field observations, including many from the Global Primary Production Data Initiative [*Olson et al.*, 2001], were compiled for this study.

[9] Observations of NPP were gathered from the literature, with the majority from the Oak Ridge National Laboratories (ORNL) Net Primary Production database (http://www-eosdis.ornl.gov/NPP/npp_home.html), and additional studies to increase the spatial and temporal coverage of the database (Table 1) [*Malhi et al.*, 2004; *Turner et al.*, 2005]. Observations from permanent pasture,

crop, wetland, or other intensively managed sites were omitted from this study; only "natural" ecosystems were included in the data set. Data were plotted using their associated geographic coordinates, and sites that fell outside of a land-sea mask were omitted from the study (Figure 2 in section 3.4). Observations that were compiled in addition to the GPPDI were subject to the minimum requirements set forth by *Olson et al.* [2001],

[10] "• the use of one or more accepted methods to estimate above- or below-ground NPP;
• specification of the geographical location for the study site;
• specification of the definition of biome or vegetation type; and
• a citable reference to peer-reviewed publication, symposium, or workshop proceedings; book chapter; or technical memorandum."

[11] Several sites (n = 393) reported only aboveground NPP. To estimate belowground NPP for these sites, we used the relationships between aboveground and belowground NPP for sites that reported measurements for both quantities reported by *Olson et al.* [2001]. A belowground NPP to total NPP ratio of 0.50 was used for nonforest biomes, and a ratio of 0.22 was used for forest biomes. *Gower et al.* [1999] reported similar values, and the forest/nonforest distinction was made by *Olson et al.* [2001] owing to a lack of statistical difference in the ratios between biome functional types.

3. Methods

[12] The suite of models presented here expands on previous studies that illustrated how climatic variables control patterns of net primary productivity [*Churkina and Running*, 1998; *King et al.*, 1997; *Lieth*, 1973; *Post et al.*, 1997]. In this paper we develop four different empirical models of NPP based on pairs of climate variables: (1) growing-season averaged photosynthetically active radiation (PAR) and a water stress index, (2) growing degree-day (base 5) and a water-stress index, (3) annual mean temperature and total annual precipitation, the variables and functional form used by *Lieth* [1973], and (4) a modified version of the *Lieth* [1973] model.

3.1. Biophysical Variables

3.1.1. Photosynthetically Active Radiation

[13] Light use efficiency models [*Montieth*, 1972, 1977] are based on the principle that canopy carbon fixation is proportional to absorbed light [*McCree*, 1972] and have been shown to be effective in modeling NPP [*Gower et al.*, 1999; *Ruimy et al.*, 1999]. We use the annual average incident photosynthetically active radiation (PAR) summed for every day that the average temperature is greater than 0°C. Adjusting PAR for times when temperatures lie above zero allows consideration of high-altitude areas, where temperatures can differ significantly from other sites at the same latitude. Preliminary analyses using our 3023 observations suggested a linear relationship between PAR and observed NPP.

3.1.2. Water Stress Index

[14] Water availability is crucial to vegetation growth [*Stephenson*, 1990]. *Rosenzweig* [1968] was the first to use actual evapotranspiration, a surrogate for moisture availability, to model NPP. Most global ecosystem models use evapotranspiration (either potential or actual) as a key element in computing the water balance [*Churkina et al.*, 1999]. Potential evapotranspiration is the rate at which evapotranspiration would occur if the soil was always wet, while actual evapotranspiration is a measure of the actual amount of water that either transpires or evaporates from plants and soil [*Churkina et al.*, 1999; *Rosenzweig*, 1968; *Stephenson*, 1998]. Here we employ a water stress index (defined as actual evapotranspiration divided by potential evapotranspiration) to gauge the ability of the land surface to satisfy the evaporative demands of the atmosphere [e.g., *Prentice et al.*, 1993; *Foley*, 1994]. Initial data analysis suggested a linear relationship between available water and NPP.

3.1.3. Growing Degree Days

[15] Growing degree-days (GDD) are often used as a surrogate to represent the length and thermal properties of the growing season [*Cramer and Solomon*, 1993]. A sufficient amount of heat during the growing season is required to drive photosynthesis reactions [*Bonan*, 2002]. The response function for GDD was designed to simulate these physiological constraints and is prescribed as a sigmoidal curve, as suggested by a preliminary analysis of GDD versus NPP.

3.2. Miami Model

[16] The Miami model is based on relationships between annual average temperature, annual precipitation, and NPP. The function that describes the relationship between precipitation and productivity is based on the Walter ratio, where the NPP for arid regions was observed to increase by 1.0 g-C m^{-2} for each millimeter of precipitation [*Lieth*, 1973]. The temperature model is based on the van't Hoff rule, which states that productivity doubles every 10°C between −10°C and 20°C [*Lieth*, 1973]. Over the past 30 years, this model has been used as a baseline data set and has been shown to yield "reasonable estimates" of global patterns of productivity [*Adams et al.*, 2004].

3.3. Input Data Derivation

[17] The biophysical variables were calculated using a simple energy and water balance model [*Foley*, 1994; *Haxeltine and Prentice*, 1996; *Prentice et al.*, 1993; *Ramankutty et al.*, 2002].

[18] Growing degree-days (GDD) were calculated as

$$GDD = \sum_{i=1}^{365} \max(0, T_i - 5) \qquad (\text{day} - \text{degrees}), \qquad (1)$$

where T_i is the daily mean temperature that is set to a (base temperature, 5°C), summed over the year.

[19] The potential evapotranspiration (PET) was calculated as

$$PET = Rn_0/\lambda^* s/(s+\gamma)(\text{mm/day}), \qquad (2)$$

where, Rn_0 is the daily net radiation, s is the rate of change of saturated water-vapor pressure with respect to tempera-

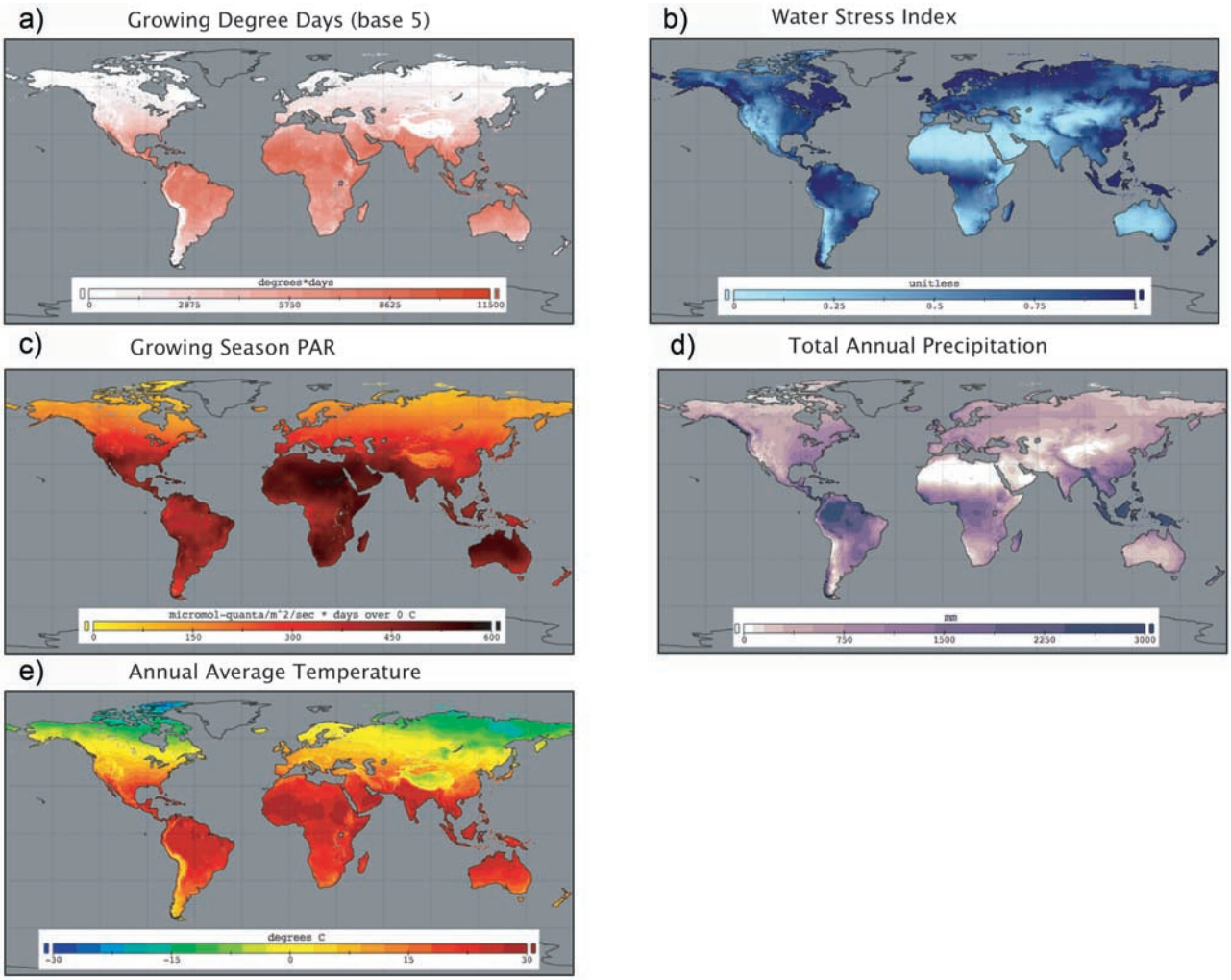

Figure 1. Model-simulated (a) growing degree-days calculated as the annual sum of daily mean temperatures over a threshold of 5°C and (b) water stress index calculated as the ratio of actual evapotranspiration to potential evapotranspiration. Values closer to zero indicate an increased water stress. (c) Average photosynthetically active radiation (PAR) during the growing season. The growing season is defined as any day with an average temperature greater than zero. (d) Total annual precipitation and (e) average annual temperature from *New et al.* [2002].

ture, γ is the psychrometer constant (65 Pa/K) and λ is the latent heat of vaporization of water (2.5×10^6 J/kg).

[20] Following the approach of *Prentice et al.* [1993], actual evapotranspiration (AET) was calculated as

$$AET = \min(PET, ET_{\max}(S_m/WC_a)) \quad \text{(mm/day)}, \quad (3)$$

where S_m is soil moisture, WC_a is available water content, and ET_{max} is the maximum daily evapotranspiration, 5.0 (mm/day).

[21] A water stress index (WSI), indicating the ability of the land surface to meet the atmospheric demand for water, was calculated as

$$WSI = AET/PET(\text{unitless}) \quad (4)$$

and is a measure of water availability to plants.

[22] The average incident photosynthetically active radiation (PAR) was summed during the growing season, which is defined as every day with an average temperature greater than zero.

[23] Observed monthly mean climate data were entered in the model at 10′ (0.1667°) latitude × longitude spatial resolution, an improvement over previous climate data sets [*New et al.*, 2002]. The monthly mean input values are interpolated to accommodate the daily time step of the model, except for evapotranspiration, which is calculated on a quasihourly time step. The model was run for 50 years to ensure that an equilibrium state was reached in the water balance submodel. The results for GDD5, WSI, and PAR are shown in Figures 1a–1c. The mean annual temperature and annual precipitation values, also derived from *New et al.* [2002], are shown in Figures 1d and 1e.

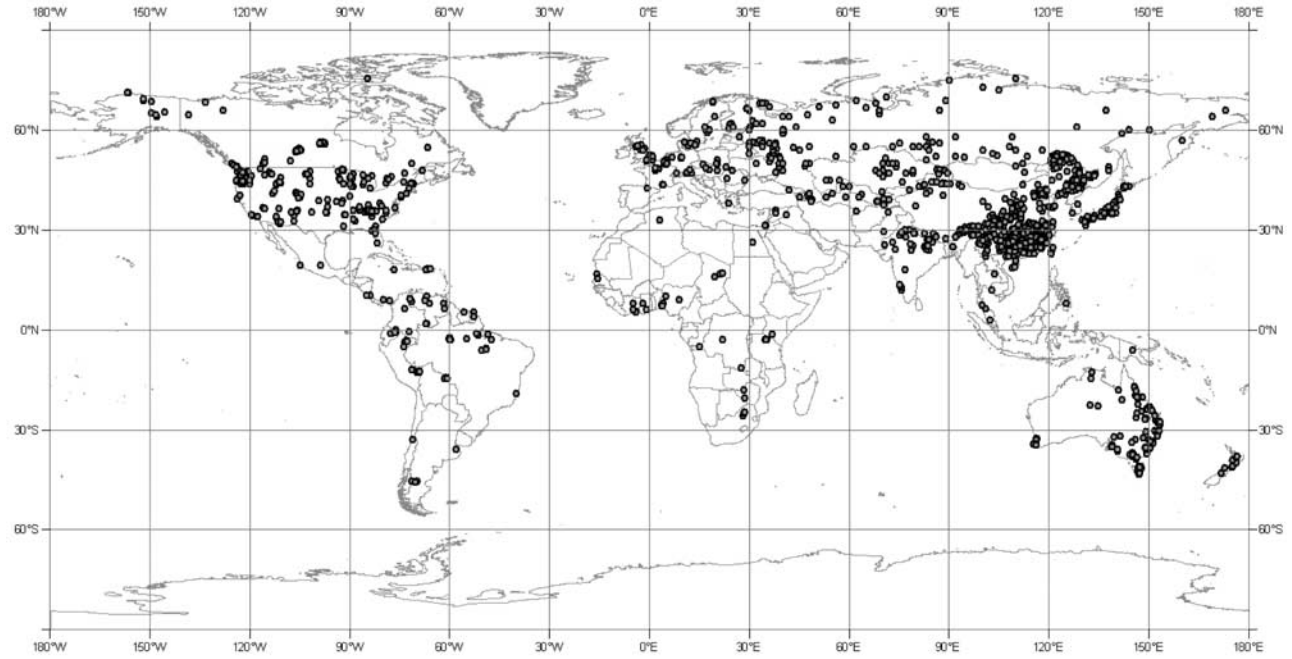

Figure 2. Spatial distribution of NPP observations collected from the ORNL DAAC NPP database (http://www-eosdis.ornl.gov/NPP/npp_home.html) and other primary literature sources. See Table 1 for all data sources used.

3.4. Empirical Models for NPP

[24] We developed statistical models between pairs of the biophysical variables and observations of NPP, as follows:

$$NPP(PAR, WSI) = \max(0, (a*PAR + b*WSI - c)), \quad (5)$$

$$NPP(GDD5, WSI) = \max(0, ((a/(1 + \exp(b - c*GDD5)) *(d*WSI - e))), \quad (6)$$

$$NPP(Temp, Precip) = ((a/1 + \exp(b - c*Temp)) *(d*(1 - (\exp e*Precip)))), \quad (7)$$

$$NPP(Temp, Precip) = \min((a/1 + \exp(b - c*Temp)), (d*(1 - \exp(e*Precip)))). \quad (8)$$

The empirical functions were designed to be linear with PAR and WSI and sigmoidal with GDD. These equations were constrained to ensure NPP values greater than zero. The temperature-precipitation model (equation (7)) used the same functional form for each variable individually as *Lieth* [1973], but uses a multiplicative form, rather than finding the limiting criterion, to combine them; this form fits the model over a surface using both independent variables. The original Miami model formulation (equation 8) was also used with updated coefficients.

[25] We then fit these equations to the observed NPP data. Unfortunately, the distribution of NPP observations is clustered in geographic space, with many observations in the Northern Hemisphere temperate latitudes and few observations in the Southern Hemisphere (Figure 2). Furthermore, within each of the 10′ grid cells of the input climate data, observed NPP varies in response to changes in microclimate, soil heterogeneity, and other factors. Ideally, functions would be fit through the entire cloud of data points, but the aforementioned variability does not allow for a good model fit. Therefore we developed a scheme to aggregate NPP observations in climate space and explicitly remove the microscale variability in NPP observations.

[26] We binned our NPP observations into a 10 × 10 matrix that described the range of climatic variables across the globe. Each axis represented one of the independent climate variables and was divided into 10 bins of equal size (Figures 3a–3c). The input climate data and observations were scaled from 0.0 to 1.0 to aid in the modeling process, and all model coefficients are given in scaled terms. NPP observations were overlaid with the 10′ resolution biophysical data and assigned to the grid. Few NPP observations were measured in extreme environments where NPP is known to be very low (i.e., deserts). Therefore, to allow the empirical model to fit accurately at low NPP values, "dummy" bins were added to the matrix where one of the climate variables was zero, and a value of zero NPP was assigned to these bins.

[27] The wide range of taxa and biological responses to climate in each climate bin, in addition to other uncertainties, add to the variability in the median NPP value in each bin. Comparing the mean across all the bins of the within-bin standard deviation to the standard deviation of the

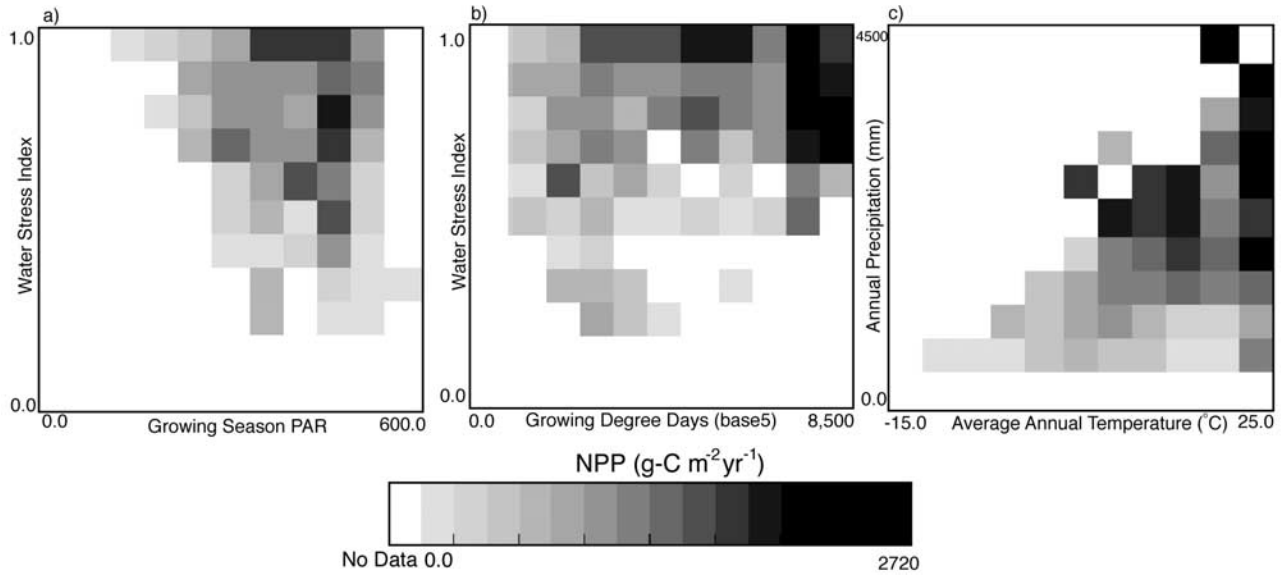

Figure 3. NPP observations binned according to climate variables: (a) growing season PAR and a water stress index, (b) growing season PAR and a water stress index, and (c) annual precipitation and average annual temperature. The median value of NPP is displayed.

median of all the climate bins revealed that about half the total variance contained in the within-bin variability (Table 2). This study does not try to explain the within-bin variance, but rather focuses on the broad-scale relationship between NPP and climate.

[28] The model coefficients were determined using a converging successive approximation approach, whereby we bisected the parameter space of each coefficient and in each iteration determined the best solution, then repeated the procedure to further refine the parameter space. Model fitting was initialized using coefficient values chosen to minimize variance in the final model output. Binned observed NPP was compared to the model output for each fitting iteration, and fits yielding acceptable slope ($0.9 < \text{slope} < 1.1$) and intercept ($0 < \text{intercept} < 0.2$) in predicted versus observed (1:1) plots were ranked according to minimization of the least squares error (Table 3). The best fitting set of coefficients was then used to update the range of acceptable values for the next fitting iteration. One hundred iterations were performed, which was sufficient for a fit to converge on stable values.

[29] Each model fit was then used in one of 500 bootstrap simulations of global NPP to determine the uncertainty of modeled NPP estimates. For each model fit, the original data set of 3023 observations was randomly sampled with replacement and then binned as described above. For each 10′ grid cell, the median NPP value from the bootstrap analysis is reported (Figures 4a–4d). The 90% confidence intervals from the Monte Carlo analyses are used for further model comparisons. Global NPP values and their 90% confidence intervals for each model type were calculated by summing the output of each of the model fits over the globe, then ranking the 500 sums and choosing the 5th percentile, median and 95th percentile values.

4. Results

[30] The modeled spatial patterns of NPP were compared to observations in order to evaluate the overall goodness of model fit. Data-poor areas, where it was impossible to validate the model, include much of the African continent, the Middle East, southern South America, western Canada, India, northern Russia, western Australia, and Southeast Asia. While we were unable to evaluate model performance over these data-poor regions, enough observations were available elsewhere for a thorough evaluation of goodness of fit.

[31] Modeled values of NPP ranged from 0 to 1577 g-C m^{-2} yr^{-1} across the three models, and the global total NPP from the median model values ranged from 41.8 to 61.3 Gt-C yr^{-1} (Table 4), which falls within the range reported by other studies summarized by *Cramer et al.* [1999]. In general, modeled values of NPP were highest in humid tropical forests, where neither water nor heat limits production. The lowest modeled values of NPP were in the desert and polar regions where sufficient quantities of water, heat or light are not available for plant production.

Table 2. Comparison of Within-Bin Standard Deviation to Between-Bin Standard Deviation Illustrating That About Half of the Total Variance is Contained in the Within-Bin Variability

	Between Bin Standard Deviation	Within Bin Standard Deviation
PAR/WSI	0.096	0.105
GDD5/WSI	0.124	0.118
Temp/Precip	0.125	0.121

Table 3. Model Coefficients Corresponding to Equations (5)–(8) and Statistical Analysis for Each Model Including Least Squared Error, Correlation Coefficient (R) With Associated Significance Level (prob), and the Slope and Intercept From a Linear Regression of Predicted Versus Observed Values

	a	b	c	d	e	LSE	R	Prob	Slope	Intercept
PAR/WSI	0.500	0.600	0.500			0.561	0.774	<0.001	0.95	0.01
GDD5/WSI	3.96	6.33	1.50	39.58	14.52	0.972	0.753	<0.001	0.90	0.01
Temp/Precip (multiplicative)	−20.13	9.50	2.25	−45.83	−3.50	0.524	0.824	<0.001	0.90	0.02
Temp/Precip (Miami)	0.50	3.75	6.34	7.50	−0.13	0.351	0.895	<0.001	0.91	0.01

[32] A histogram of productivity by area illustrates the general patterns of global NPP (Figure 5). All the models produced nonnormal frequency distributions of NPP, with more low-productivity area and less high productivity area. There are comparatively few low NPP values in the PAR/WSI model, while more area is occupied by the midrange values (400–800 g-C m^{-2} yr^{-1}). The Temp/Precip (Miami) generally has higher values than the Temp/Precip (multiplicative) model although its maximum NPP value is only ~1100 g-C m^{-2} yr^{-1}. This nonspatially explicit interpretation of global NPP is complemented by the biome and zonal averages.

4.1. Zonal Averages

[33] The observations and model results were sorted into 2.5° latitude bands and averages for each were calculated for those that contained greater than five observations (Figure 6a). Observations cover the range of −47.5° to 75°, while the land surface extends from −55° to 85°. When comparing observations to modeled NPP using zonal aver-

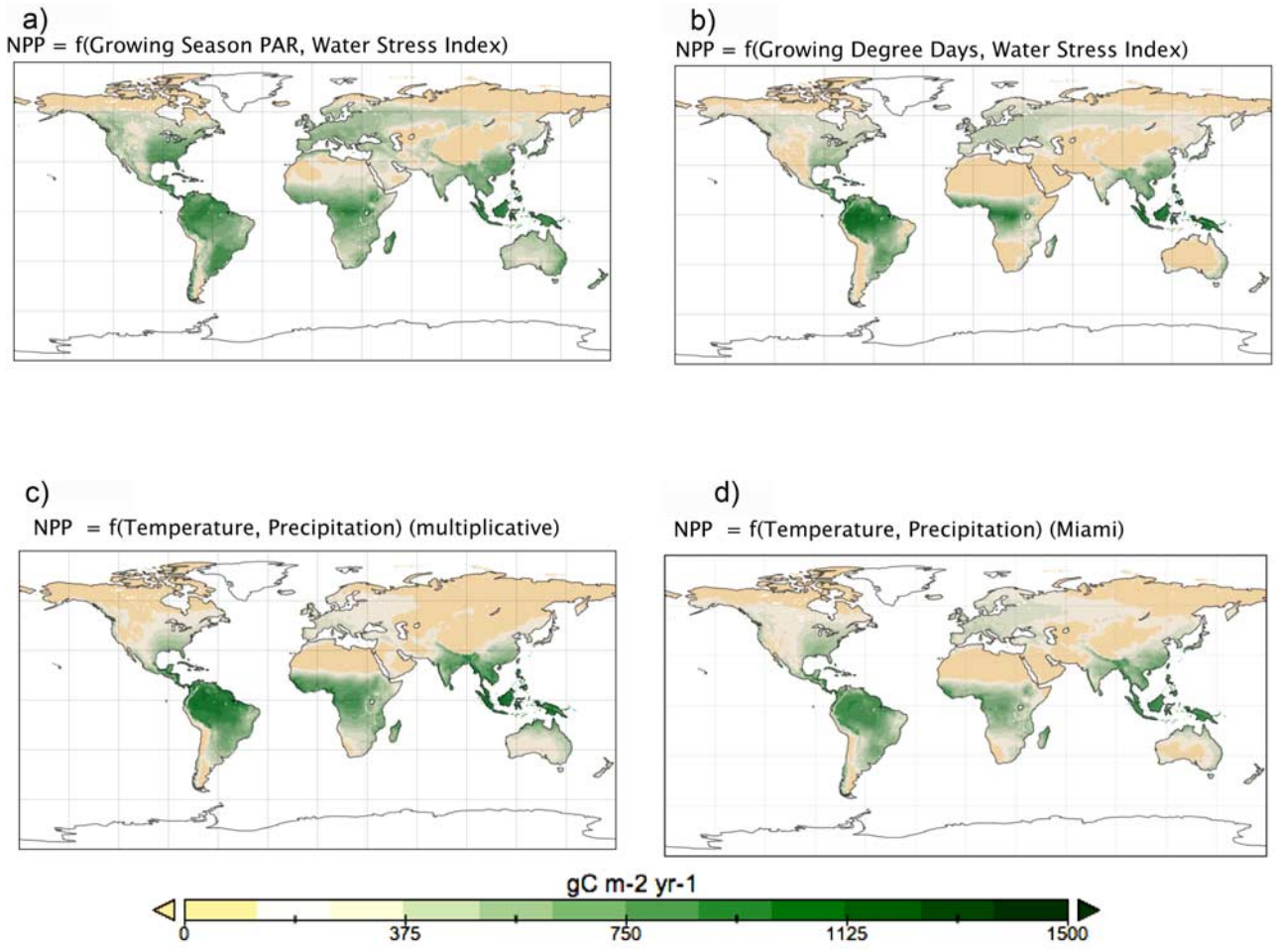

Figure 4. Net primary productivity as a function of (a) growing season PAR and water stress index, (b) growing degree-days (base 5) and water stress index, (c) annual average temperature and annual precipitation (multiplicative), and (d) annual average temperature and annual precipitation (Miami). Global NPP for these models are 61.3 (55.6, 73.9) GtC, 41.8 (39.2, 44.6) GtC, 52.0 (47.3, 54.7) GtC, and 45.1 (36.5, 51.7) respectively. Values in parentheses bound the 90% confidence interval.

Table 4. Global Total NPP, Uncertainty in Global Total NPP, Maximum Modeled NPP Value, and Percent Agreement Between Modeled NPP and Observations

	Median Global NPP, Gt-C	90% Confidence Interval		Maximum Modeled NPP, g-C m^{-2} yr^{-1}
		5th Percentile	95th Percentile	
Growing season PAR–water stress index	61.3	55.6	73.9	1577
Growing degree days–water stress index	41.8	39.2	44.6	1559
Temp/Precip (multiplicative)	52.0	47.3	54.7	1561
Temp/Precip (Miami)	45.1	36.5	51.7	1164

ages, the widely distributed network of points allows for comparison to modeled results. Zonal-average model results follow the general latitudinal trends of the observations, with NPP decreasing from the equator to the poles. In most areas, the models simulated the observations well, but in other areas, the patterns of modeled NPP differed from the expected results. We believe that this is simply a result of the insufficient spatial coverage of the observations.

[34] The observations around −40° are dominated by a cluster of points in New Zealand and southern Australia that report NPP values higher than expected for the region. Most of these observations come from the temperate broadleaf evergreen and grassland biomes. In addition, there are no other observations in that latitude band, therefore the unexpectedly high observations are not moderated by lower values that would be found at that latitude in South America.

[35] All models exhibited peak NPP values at the equator, however, observed data decreased from both −2.5° and 2.5° to 0°. While observations in this latitude band did not correspond to the modeled NPP, there were likely other observations in the same climate matrix cell that acted to increase the modeled NPP values for this area. Averaging grid cells over 2.5° latitude bands for the whole land surface allows for comparison of general trends between models (Figure 6b). NPP for all models exhibited a trimodal distribution consistent with other studies [*Kicklighter et al.*, 1999].

[36] The slight peak in NPP at −55° corresponds to the very southern tip of South America, where there is sufficient light and water for plant growth. Other latitude bands were averaged over larger areas, and this slight peak can be attributed to the small land area in this band. All models increase to their peak NPP at the equator. The PAR/WSI model has the lowest peak, and this can be attributed to a reduction in PAR due to an increase in cloud cover, and hence, a decrease in NPP. All models decrease from their peaks at the equator, as deserts dominate the land surface

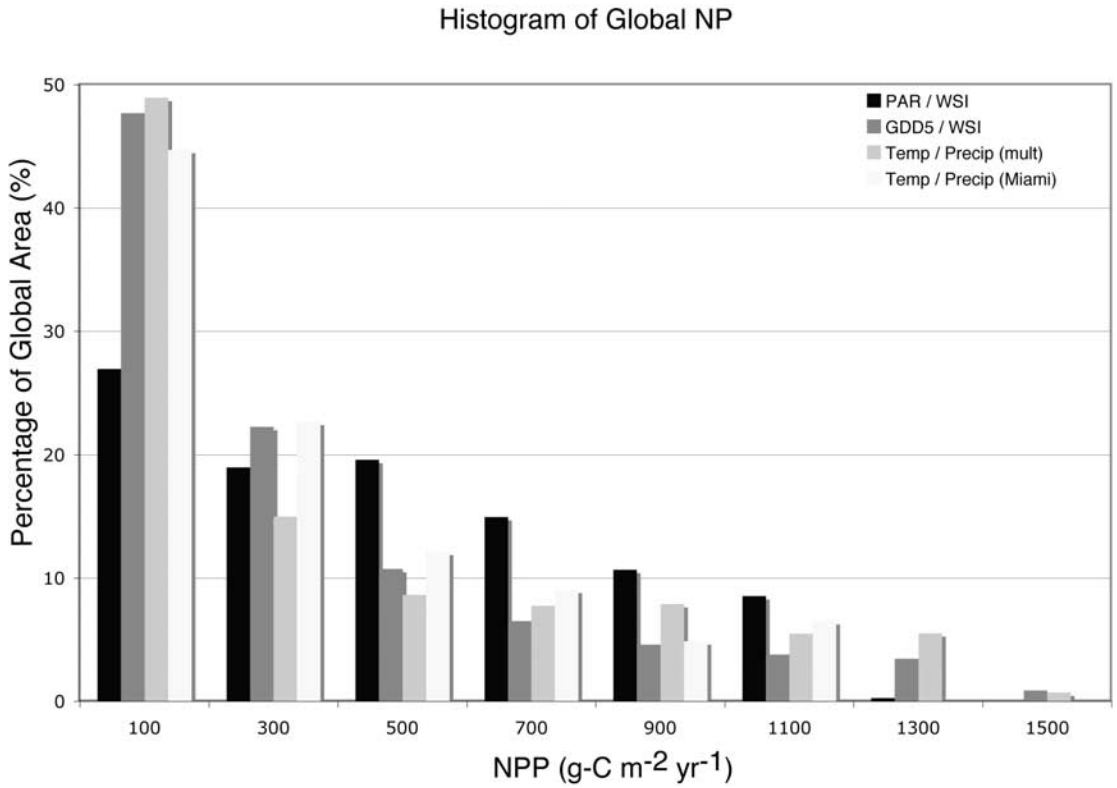

Figure 5. Histogram of NPP values binned by 200 units of NPP. There is a general trend of more area occupied by less productive land occupied by highly productive land.

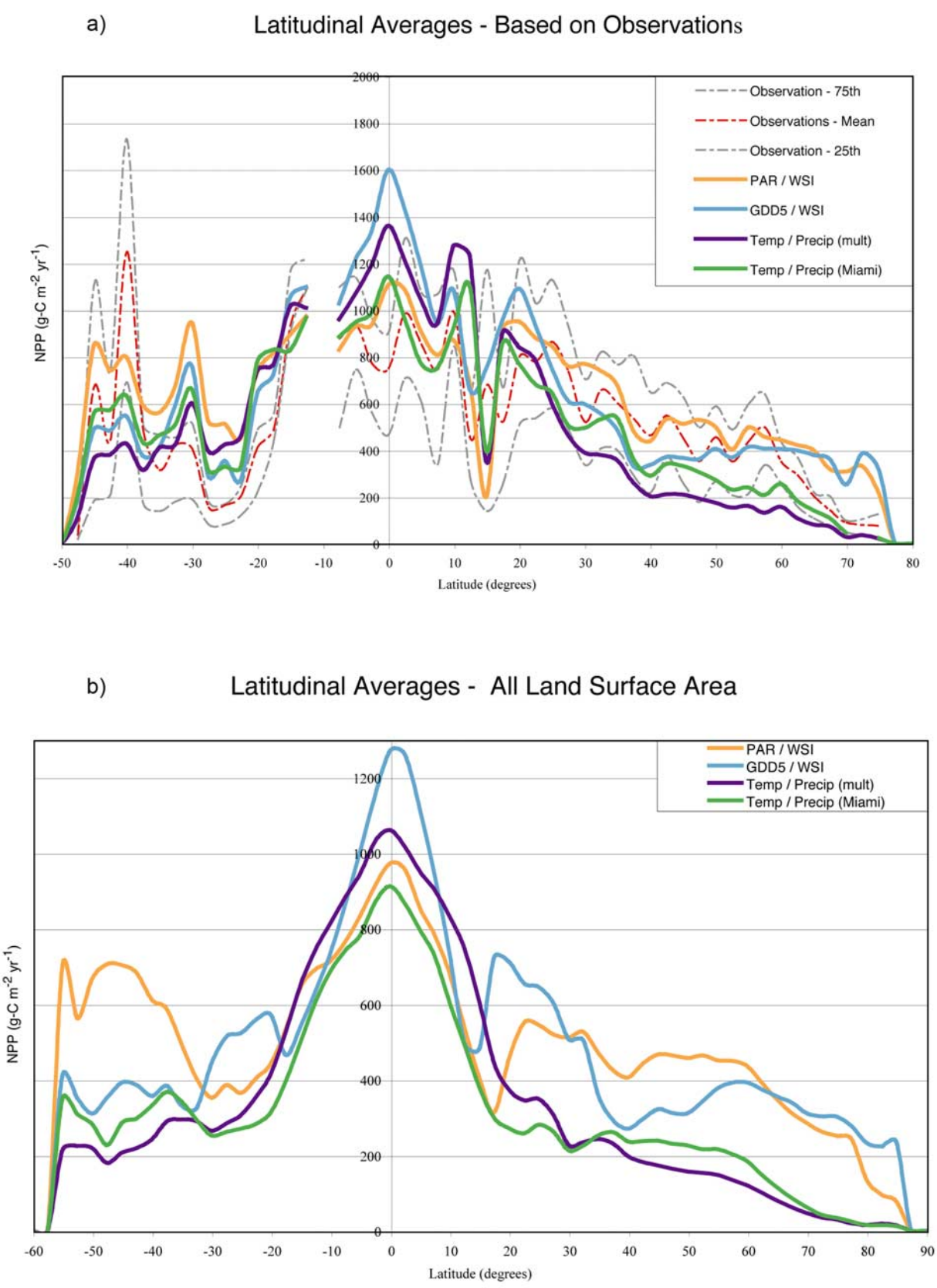

Figure 6. (a) Median and quartile observed NPP for each 2.5° latitude band that contained observed data (dashed lines) and comparison of modeled NPP in cells with observed data (solid lines) and (b) average modeled NPP over 2.5 latitude bands for all grid cells.

around 20°. The PAR/WSI and GDD/WSI models increase in NPP and peak at 55° as the water availability and PAR or GDD are sufficient for plant growth, but the Temp/Precip model NPP declines in magnitude until 90°.

4.2. Biome Averages

[37] A classification of global vegetation biomes by *Ramankutty and Foley* [1999] defined 15 biomes on the basis of potential natural vegetation. The quartiles for the observations of NPP by each biome are displayed along with our NPP model estimates for grid cells that contain observations (Figure 7a) and over the whole land surface (Figure 7b). Bounds of the 90% confidence intervals (5th and 95th percentiles)in the modeled NPP are shown for each biome. There are no observations from the polar desert/rock/ice biome, and therefore it is not included in the figures. NPP tends to be higher in the forested biomes, with the highest zonal averages occurring in the tropical forest biomes, followed by the temperate forest biomes. The lowest modeled NPP values occur in nonforest biomes: open shrubland, tundra, and desert.

[38] Model output falls within the bounds of the observations for most biomes. In the boreal deciduous forest/woodland and tundra biomes, both forms of the Temp/Precip model underpredicts NPP, as they generally predict low values in northern latitudes. The GDD/WSI model underpredicts NPP in the desert biome. This can be attributed to the functional form of the equation, and NPP is modeled to be zero in most high-latitude and desert areas.

[39] In both tropical biomes, the PAR/WSI model returns the lowest NPP. In the three temperate biomes the PAR/WSI model reports the highest NPP, and in most cases, the Temp/Precip models report the lowest values. In the nonforest biomes, the general trend (from highest NPP to lowest) is PAR/WSI, GDD/WSI, Temp/Precip (Miami), Temp/Precip (multiplicative).

[40] When NPP is averaged across the entire land surface, the general trends remain constant, with the exception of a few biomes (Figure 7b). In general, when averaged over a larger area, the magnitude of NPP is lower for all biomes, when compared to averaging only over grid cells with observations. With the exception of the boreal biomes, forested biomes have higher NPP than nonforest biomes.

5. Discussion/Conclusion

[41] Net primary production is one of the fundamental characteristics of the biosphere, providing usable energy for life on Earth. However, our knowledge of the geographic patterns of NPP around the planet is still limited. Advancements in field measurements of NPP and associated biophysical variables over the last several decades have allowed for models of biospheric processes to be developed and tested. In this paper, we have demonstrated that global patterns of NPP can be reasonably predicted using empirical models based on simple pairs of biophysical and climatic variables. These models allow us to gain an understanding of the global patterns of NPP.

[42] While there is still a great deal of variability, all the models performed within expected bounds with respect to global totals of NPP and spatial distribution across biomes and latitude zones. The PAR/WSI and GDD/WSI models seem to represent most closely the physiological limitations on plants that ultimately affect their NPP. The Temp/Precip models, used to retest the hypothesis of *Lieth* [1973], also captured the drivers of global-scale NPP.

[43] While our study has taken a step forward in developing models of global patterns of NPP, there are still many caveats that need to be addressed. First, observations of NPP in the field are plagued by numerous problems. Some authors have pointed to inconsistencies in the functional definition of NPP [*Roxburgh et al.*,2005], while others have criticized the "incomplete or inappropriate" methods of field measurement [*Clark et al.*, 2001a]. NPP is most commonly reported as an annual flux, and those measurements are difficult to obtain, even over small areas [*Cramer et al.*, 2001a]. *Clark et al.* [2001a] argued that in situ NPP calculations (for forests) should be based on the aggregation of above and below ground coarse woody increment in addition to litterfall, insect damage, fruit production, and root exudates. However, the time and money required to collect data of that quality over a large spatial scale are prohibitive. In addition, early estimates of NPP, such as those from the International Biosphere Programme (IBP) used less sophisticated methodologies and may underestimate both above and belowground stocks of carbon [*Clark et al.*, 2001a].

[44] There is also a discrepancy between the scale of our model simulations and the NPP observations. The size of a 10′ grid cell at the equator is 345 km^2, while the average size of a field study is often several hectares or less. Local observations of NPP are influenced by landscape heterogeneity, including changes in microclimate and soil fertility due to land use, historical patterns of disturbance, successional stage, altitudinal gradients, and hydrology. Using a Monte-Carlo analysis allowed for calculation of confidence intervals of the median NPP value for each grid cell.

[45] Another obstacle of using such a large and diverse database of observations is the time period in which the observations have been taken. From the IBP studies of the 1960s–1970s to the most recent MODIS BigFoot validation efforts from 1999–2003, both atmospheric carbon dioxide concentrations and global patterns of climate have changed [*Intergovernmental Panel on Climate Change*, 2001]. These changes have the potential to impact the physiological and ecological responses of plants, making the observations of NPP from different time periods functionally incompatible. The climate data used by *New et al.* [2002] to derive the biophysical variables are 30-year averages (1961–1990) and do not cover the full time range of the observations.

[46] In order to quantify NPP over large spatial scales, methods beyond direct observation must be used. Several space-borne sensors (i.e., MODIS, AVHRR, Landsat) record reflectance values from vegetation that can be processed, through biophysical models like those described here, to estimate NPP [*Bradford et al.*, 2005; *Goetz and Prince*, 1996; *Turner et al.*, 2005]. However, the raw reflectance data must still be calibrated to on-the-ground measurements in order to train the algorithms, as reflectance is not a direct measurement of productivity. Flux tower

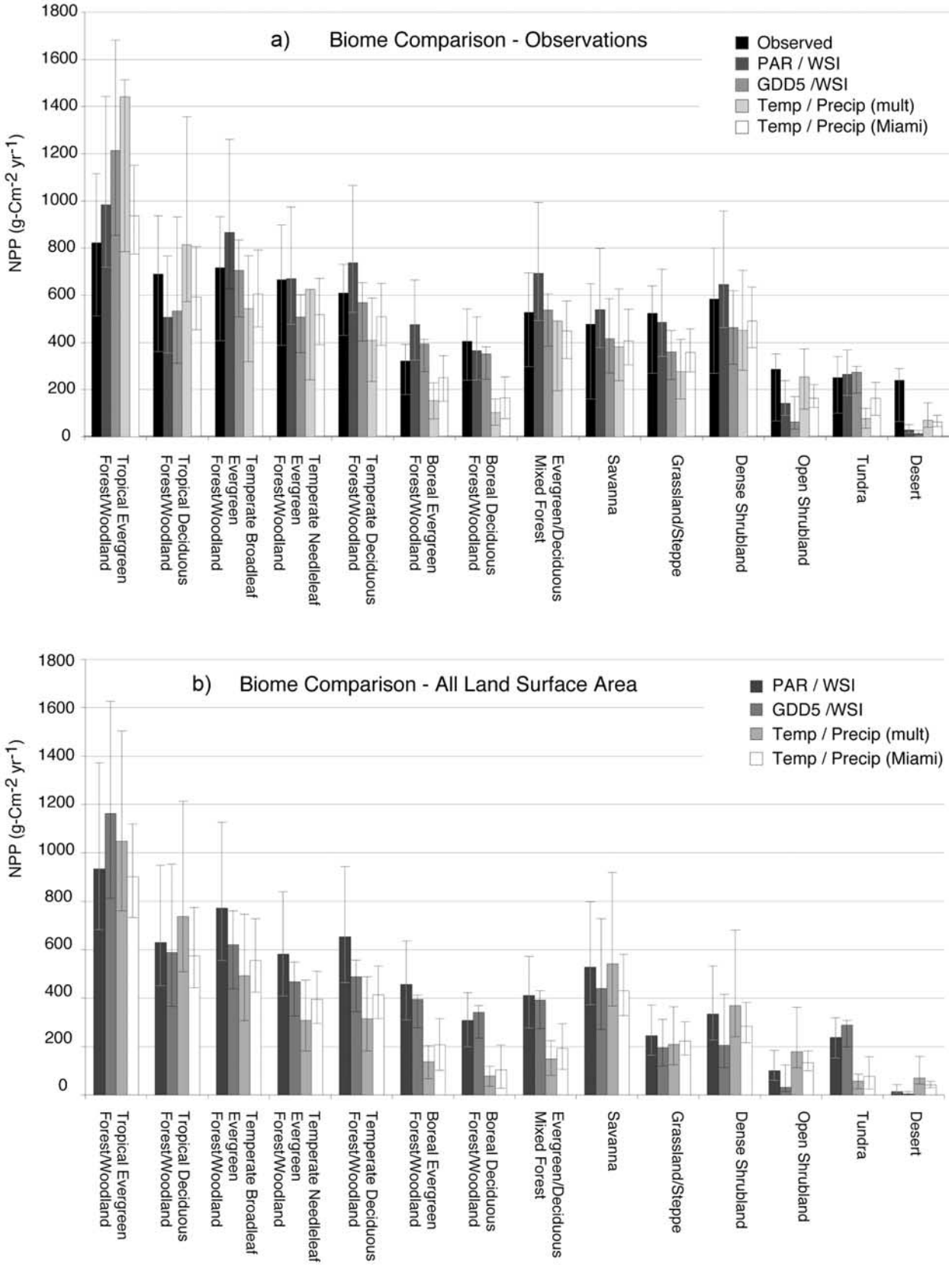

Figure 7. Average NPP over 14 biomes. Biomes defined by *Ramankutty and Foley* [1999]. (a) Models averaged only over cells with observations and (b) models averaged over all grid cells.

measurement sites also report NPP [*Hibbard et al.*, 2005], but the methods of standardization for these sites is ongoing and their spatial distribution is too limited for incorporation into this study.

[47] While the general patterns of NPP were similar between the four models, the magnitude and distribution varied sufficiently to warrant further investigation. The mathematical form of the model equations had some unintended consequences when applied globally. In the models that used sigmoidal equations, even if the independent variable was zero, modeled NPP would nevertheless have a small positive value. For example, if a grid cell had zero growing-degree days, NPP would still never be exactly zero. In addition, in the models that used the water stress index, the linear form of the equation included an intercept that produced negative NPP for highly water stressed areas; in these cases the model would predict a negative NPP, but was constrained to have values of zero or higher.

[48] This study reports the potential NPP of the world's ''natural'' ecosystems and excludes managed areas such as crops, pastures, and plantations. The NPP of modified landscapes can vary dramatically owing to irrigation, fertilization, grazing, and other alterations to natural systems. NPP of such systems has been calculated [*Hicke and Lobell*, 2004; *Prince et al.*, 2001] in a broader attempt to determine the human impact on the biosphere [*Imhoff et al.*, 2004; *Vitousek et al.*, 1997].

[49] The Miami model [*Lieth*, 1973] was a major achievement in understanding global patterns of productivity, but more observations and new hypotheses about the climatic controls on NPP call for reanalysis of the problem. We developed four empirical models in order to extend a finite database of NPP observations to describe global patterns of NPP. We found that the PAR/WSI model performed the best, followed by the GDD/WSI and Temp/Precip models.

[50] This study strengthens our understanding of global productivity and will allow for improved ecosystem model evaluation. Standardization of field measurement techniques to quantify changes in ecosystem productivity and functioning is needed, in addition to a greater number of study sites. Further work on incorporating these global networks of field measurements into global ecosystem models could help reduce uncertainties in our understanding of the biospheric response to land use and changing climate.

[51] **Acknowledgments.** We would like to thank C. Kucharik, S. Olson, and E. Sowatzke for their support. This work was supported by NASA Terrestrial Ecology grant (NAG5-13351). Supplemental material will be posted at http://www.sage.wisc.edu.

References

Adams, B., A. White, and T. M. Lenton (2004), An analysis of some diverse approaches to modelling terrestrial net primary productivity, *Ecol. Modell.*, *177*, 353–391.

Benitez, P. C., I. McCallum, M. Obersteiner, and Y. Yamagata (2007), Global potential for carbon sequestration: Geographical distribution, country risk and policy implications, *Ecol. Econ.*, *60*(3), 572–583.

Bonan, G. B. (2002), *Ecological Climatology: Concepts and Applications*, 678 pp., Cambridge Univ. Press, New York.

Bradford, J. B., J. A. Hicke, and W. K. Lauenroth (2005), The relative importance of light-use efficiency modifications from environmental conditions and cultivation for estimation of large-scale net primary productivity, *Remote Sens. Environ.*, *96*, 246–255.

Churkina, G., and S. W. Running (1998), Contrasting climatic controls on the estimated productivity of global terrestrial biomes, *Ecosystems*, *1*, 206–215.

Churkina, G., S. W. Running, and A. L. Schloss (1999), Comparing global models of terrestrial net primary productivity (NPP): The importance of water availability, *Global Change Biol.*, *5*, 46–55.

Clark, D. A., S. Brown, D. W. Kicklighter, J. Q. Chambers, J. R. Thomlinson, and J. Ni (2001a), Measuring net primary production in forests: Concepts and field methods, *Ecol. Appl.*, *11*, 356–370.

Clark, D. A., S. Brown, D. W. Kicklighter, J. Q. Chambers, J. R. Thomlinson, J. Ni, and E. A. Holland (2001b), Net primary production in tropical forests: An evaluation and synthesis of existing field data, *Ecol. Appl.*, *11*, 371–384.

Cramer, W., and C. B. Field (1999), Comparing global models of terrestrial net primary productivity (NPP): Introduction, *Global Change Biol.*, *5*, III–IV.

Cramer, W., and A. Solomon (1993), Climatic classification and future global redistribution of agricultural lands, *Clim. Res.*, *3*, 97–110.

Cramer, W., B. Moore, and D. Sahagian (1996), Data needs for modelling global biospheric carbon fluxes: Lessons from a comparison of models, *IGBP Newsl.*, *27*, 13–15.

Cramer, W., D. W. Kicklighter, A. Bondeau, B. Moore, C. Churkina, B. Nemry, A. Ruimy, and A. L. Schloss (1999), Comparing global models of terrestrial net primary productivity (NPP): Overview and key results, *Global Change Biol.*, *5*, 1–15.

Cramer, W., et al. (2001a), Global response of terrestrial ecosystem structure and function to CO_2 and climate change: Results from six dynamic global vegetation models, *Global Change Biol.*, *7*, 357–373.

Cramer, W., R. J. Olson, S. Prince, J. M. O. Scurlock, and Members of the Global Primary Production Data Initiative (2001b), Determining present patterns of global productivity, in *Terrestrial Global Productivity*, edited by J. Roy, B. Saugier, and H. A. Mooney, pp. 429–448, Academic Press, San Diego, Calif.

DeFries, R. S., C. B. Field, I. Fung, G. J. Collatz, and L. Bounoua (1999), Combining satellite data and biogeochemical models to estimate global effects of human-induced land cover change on carbon emissions and primary productivity, *Global Biogeochem. Cycles*, *13*, 803–815.

Foley, J. A. (1994), Net primary productivity in the terrestrial biosphere: The application of a global model, *J. Geophys. Res.*, *99*, 20,773–20,783.

Foley, J. A., I. C. Prentice, N. Ramankutty, S. Levis, D. Pollard, S. Sitch, and A. Haxeltine (1996), An integrated biosphere model of land surface processes, terrestrial carbon balance, and vegetation dynamics, *Global Biogeochem. Cycles*, *10*, 603–628.

Goetz, S. J., and S. D. Prince (1996), Remote sensing of net primary production in boreal forest stands, *Agric. For. Meteorol.*, *78*, 149–179.

Gower, S. T., C. J. Kucharik, and J. M. Norman (1999), Direct and indirect estimation of leaf area index, f (APAR), and net primary production of terrestrial ecosystems, *Remote Sens. Environ.*, *70*, 29–51.

Gower, S. T., O. Krankina, R. J. Olson, M. Apps, S. Linder, and C. Wang (2001), Net primary production and carbon allocation patterns of boreal forest ecosystems, *Ecol. Appl.*, *11*, 1395–1411.

Haberl, H., et al. (2004), Human appropriation of net primary production and species diversity in agricultural landscapes, *Agric. Ecosyst. Environ.*, *102*, 213–218.

Haxeltine, A., and I. C. Prentice (1996), BIOME3: An equilibrium terrestrial biosphere model based on ecophysiological constraints, resource availability, and competition among plant functional types, *Global Biogeochem. Cycles*, *10*, 693–709.

Hibbard, K. A., B. E. Law, M. Reichstein, and J. Sulzman (2005), An analysis of soil respiration across Northern Hemisphere temperate ecosystems, *Biogeochemistry*, *73*, 29–70.

Hicke, J. A., and D. B. Lobell (2004), Spatiotemporal patterns of cropland area and net primary production in the central United States estimated from USDA agricultural information, *Geophys. Res. Lett.*, *31*, L20502, doi:10.1029/2004GL020927.

Imhoff, M. L., L. Bounoua, T. Ricketts, C. Loucks, R. Harriss, and W. T. Lawrence (2004), Global patterns in human consumption of net primary production, *Nature*, *429*, 870–873.

Intergovernmental Panel on Climate Change (2001), *Climate Change 2001: Synthesis Report. A Contribution of Working Groups I, II, and III to the Third Assessment Report of the Intergovernmental Panel on Climate Change*, edited by R. T. Watson and D. L. Albritton, 397 pp., Cambridge Univ. Press, New York.

Kicklighter, D. W., A. Bondeau, A. L. Schloss, J. Kaduk, and A. D. McGuire (1999), Comparing global models of terrestrial net primary productivity (NPP): Global pattern and differentiation by major biomes, *Global Change Biol.*, *5*, 16–24.

King, A. W., W. M. Post, and S. D. Wullschleger (1997), The potential response of terrestrial carbon storage to changes in climate and atmospheric CO_2, *Clim. Change*, *35*, 199–227.

Kucharik, C. J., J. A. Foley, C. Delire, V. A. Fisher, M. T. Coe, J. D. Lenters, C. Young-Molling, N. Ramankutty, J. M. Norman, and S. T. Gower (2000), Testing the performance of a Dynamic Global Ecosystem Model: Water balance, carbon balance, and vegetation structure, *Global Biogeochem. Cycles*, *14*, 795–825.

Lieth, H. (1973), Primary production: Terrestrial ecosystems, *Human Ecol.*, *1*, 303–332.

Lieth, H., and R. H. Whittaker (1975), *Primary Productivity of the Biosphere*, 339 pp., Springer, New York.

Malhi, Y., et al. (2004), The above-ground coarse wood productivity of 104 Neotropical forest plots, *Global Change Biol.*, *10*, 563–591.

McCree, K. J. (1972), The action spectrum, absorption, and quantum yield of photosynthesis in crop plants, *Agric. Meteorol.*, *9*, 191–216.

Meyerson, L. A., J. Baron, J. M. Melillo, R. J. Naiman, R. I. O'Malley, G. Orians, M. A. Palmer, A. S.P. Pfaff, S. W. Running, and O. E. Sala (2005), Aggregate measures of ecosystem services: Can we take the pulse of nature?, *Front. Ecol. Environ.*, *3*, 56–59.

Montieth, J. (1972), Solar radiation and productivity in tropical ecosystems, *J. Appl. Ecol.*, *9*, 747–766.

Montieth, J. (1977), Climate and efficiency of crop production in Britain, *Philos. Trans. R. Soc., Ser. B*, *281*, 277–294.

New, M., D. Lister, M. Hulme, and I. Makin (2002), A high-resolution data set of surface climate over global land areas, *Clim. Res.*, *21*, 1–25.

Olson, R. J., K. Johnson, D. L. Zheng, and J. M. O. Scurlock (2001), Global and regional ecosystem modeling: Databases of model drivers and validation measurements, *ORNL/TM-2001/196*, 95 pp., Environ. Sci. Div., Oak Ridge Natl. Lab., Oak Ridge, Tenn.

Post, W. M., A. W. King, and S. D. Wullschleger (1997), Historical variations in terrestrial biospheric carbon storage, *Global Biogeochem. Cycles*, *11*, 99–109.

Prentice, I. C., M. T. Sykes, and W. Cramer (1993), A simulation-model for the transient effects of climate change on forest landscapes, *Ecol. Modell.*, *65*, 51–70.

Prince, S. D., J. Haskett, M. Steininger, H. Strand, and R. Wright (2001), Net primary production of US Midwest croplands from agricultural harvest yield data, *Ecol. Appl.*, *11*, 1194–1205.

Ramankutty, N., and J. A. Foley (1999), Estimating historical changes in global land cover: Croplands from 1700 to 1992, *Global Biogeochem. Cycles*, *13*, 997–1027.

Ramankutty, N., J. A. Foley, J. Norman, and K. McSweeney (2002), The global distribution of cultivable lands: Current patterns and sensitivity to possible climate change, *Global Ecol. Biogeogr.*, *11*, 377–392.

Rosenzweig, M. (1968), Net primary production of terrestrial communities: Prediction from climatological data, *Am. Nat.*, *102*, 67–73.

Roxburgh, S. H., et al. (2004), A critical overview of model estimates of net primary productivity for the Australian continent, *Funct. Plant Biol.*, *31*, 1043–1059.

Roxburgh, S. H., S. L. Berry, T. N. Buckley, B. Barnes, and M. L. Roderick (2005), What is NPP? Inconsistent accounting of respiratory fluxes in the definition of net primary production, *Funct. Ecol.*, *19*, 378–382.

Ruimy, A., L. Kergoat, and A. Bondeau (1999), Comparing global models of terrestrial net primary productivity (NPP): Analysis of differences in light absorption and light-use efficiency, *Global Change Biol.*, *5*, 56–64.

Running, S. W., R. R. Nemani, F. A. Heinsch, M. S. Zhao, M. Reeves, and H. Hashimoto (2004), A continuous satellite-derived measure of global terrestrial primary production, *Bioscience*, *54*, 547–560.

Schlapfer, F., and B. Schmid (1999), Ecosystem effects of biodiversity: A classification of hypotheses and exploration of empirical results, *Ecol. Appl.*, *9*, 893–912.

Scurlock, J. M.O., W. Cramer, R. J. Olson, W. J. Parton, and S. D. Prince (1999), Terrestrial NPP: Toward a consistent data set for global model evaluation, *Ecol. Appl.*, *9*, 913–919.

Scurlock, J. M.O., K. Johnson, and R. J. Olson (2002), Estimating net primary productivity from grassland biomass dynamics measurements, *Global Change Biol.*, *8*, 736–753.

Sitch, S., et al. (2003), Evaluation of ecosystem dynamics, plant geography and terrestrial carbon cycling in the LPJ dynamic global vegetation model, *Global Change Biol.*, *9*, 161–185.

Steffen, W., et al. (1998), The terrestrial carbon cycle: Implications for the Kyoto Protocol, *Science*, *280*, 1393–1394.

Stephenson, N. L. (1990), Climatic control of vegetation distribution—The role of the water-balance, *Am. Nat.*, *135*, 649–670.

Stephenson, N. L. (1998), Actual evapotranspiration and deficit: biologically meaningful correlates of vegetation distribution across spatial scales, *J. Biogeogr.*, *25*, 855–870.

Turner, D. P., et al. (2005), Site-level evaluation of satellite-based global terrestrial gross primary production and net primary production monitoring, *Global Change Biol.*, *11*, 666–684.

Vitousek, P. M., H. A. Mooney, J. Lubchenco, and J. M. Melillo (1997), Human domination of Earth's ecosystems, *Science*, *277*, 494–499.

Whittaker, R. H., and G. E. Likens (1975), Primary production: The biosphere and man, in *Primary Productivity of the Biosphere*, edited by H. Lieth and R. Whittaker, pp. 305–328, Springer, Berlin.

Zhao, M. S., F. A. Heinsch, R. R. Nemani, and S. W. Running (2005), Improvements of the MODIS terrestrial gross and net primary production global data set, *Remote Sens. Environ.*, *95*, 164–176.

C. Barford, J. A. Foley, and D. P. M. Zaks, Center for Sustainability and the Global Environment (SAGE), Nelson Institute for Environmental Studies, University of Wisconsin, 1710 University Avenue, Madison, WI 53726, USA.(zaks@wisc.edu)

N. Ramankutty, Department of Geography, McGill University, 805 Sherbrooke Street W., Montreal, QC, Canada H3A 2K6.